Journal of Zhejiang University-SCIENCE B (Biomedicine & Biotechnology)
ISSN 1673-1581 (Print); ISSN 1862-1783 (Online)
www.zju.edu.cn/jzus; www.springerlink.com
E-mail: jzus@zju.edu.cn

Developing a rat model of dilated cardiomyopathy with improved survival*#

Li-juan SHEN[1], Shu LU[†‡1], Yong-hua ZHOU[†‡2], Lan LI[3], Qing-min XING[1], Yong-liang XU[2]

([1]*Wuxi Hospital of Traditional Chinese Medicine, Wuxi Hospital Affiliated to Nanjing University of Chinese Medicine, Wuxi 214071, China*)

([2]*Jiangsu Institute of Parasitic Diseases, Key Laboratory on Technology for Parasitic Disease Prevention and Control, Ministry of Health, Jiangsu Provincial Key Laboratory on Molecular Biology of Parasites, Jiangsu Provincial Key Subject on Parasitic Diseases, Wuxi 214064, China*)

([3]*Department of Ultrasonography, Wuxi Hospital of Traditional Chinese Medicine, Wuxi Hospital Affiliated to Nanjing University of Chinese Medicine, Wuxi 214071, China*)

[†]E-mail: Panda55007@163.com; toxo2001@163.com

Received June 8, 2016; Revision accepted Aug. 19, 2016; Crosschecked Nov. 10, 2016

Abstract: To compare the continuous infusion and intermittent bolus injection administration protocols of doxorubicin (Dox) under the same cumulative dose (12 mg/kg), and establish a rat dilated cardiomyopathy model with improved survival, a total of 150 Sprague-Dawley (SD) rats were divided into three groups: a control group, administered with normal saline; a Dox 1 group, administration twice a week at 1 mg/kg; a Dox 2, administration once a week at 2 mg/kg. Mortality rates in the Dox 1 and Dox 2 groups were 22% and 48%, respectively (P<0.05). As shown by echocardiography, both Dox groups exhibited significant chamber dilatation and reduced cardiac function (all P<0.05 vs. control). Plasma brain natriuretic peptide and C-reactive protein concentrations were significantly increased (P<0.05) with both Dox regimens. The concentrations of Caspase-3 in myocardial tissues of rats significantly increased in both doxorubicin regimens. Myocardial metabolism imaging by histology and ^{18}F-fluoro-deoxyglucose-positron emission tomography (^{18}FDG-PET) both revealed decreased myocardial viability and necrosis, and even interstitial fibrosis, in left ventricles (LVs) in both Dox groups. Serum creatinine and aspartate aminotransferase concentrations were significantly higher in the Dox 2 model than in the Dox 1 model. Doxorubicin given at both regimens induced dilated cardiomyopathy, while its administration at lower doses with more frequent infusions reduced the mortality rate.

Key words: Doxorubicin, Dilated cardiomyopathy, Animal model, ^{18}FDG-PET
http://dx.doi.org/10.1631/jzus.B1600257 **CLC number:** R542.2

1 Introduction

Dilated cardiomyopathy (DCM) is a common side effect complication of cancer chemotherapy (Vejpongsa and Yeh, 2014). Doxorubicin cardiotoxicity-induced DCM is characterized by chamber dilation and cardiac dysfunction, and prognosis is poor (Plana *et al*., 2014). In cancer patients who survive for five years, approximately one in three patients die from cardiovascular disease. Attempts have been made to identify risk factors, lessen the use of toxic chemotherapeutic derivatives, or detect subclinical toxicity at earlier stages. Despite these attempts, there is no current consensus on the best approach to prevent cardiotoxicity from chemotherapeutic agents. Studies on new therapeutic modalities to prevent or reverse DCM have attracted much attention. These include the use of drugs or stem cells. Reliable experimental

‡ Corresponding authors

* Project supported by the Medical Technology Major Projects on Hospital Management Center in Wuxi City, Jiangsu Province (No. YGZX1102), China

Electronic supplementary materials: The online version of this article (http://dx.doi.org/10.1631/jzus.B1600257) contains supplementary materials, which are available to authorized users

ORCID: Li-juan SHEN, http://orcid.org/0000-0001-6401-3220

models for identifying new targets and testing new treatments are needed.

Doxorubicin is a common antineoplastic agent of the anthracycline group that was isolated from fungal cultures of *Streptomyces peucetius* var. (Carvalho *et al*., 2009). Doxorubicin has a special affinity for the myocardium, and can induce DCM and congestive heart failure in cancer patients. Once congestive heart failure is diagnosed, the five year mortality rate becomes 50%. Reliable models of DCM using doxorubicin as the inducer are needed to better understand the mechanisms involved.

A DCM model was successfully established by intraperitoneally injecting rats with doxorubicin at a dose of 2 mg/kg once a week for six weeks (Turakhia *et al*., 2007). A previous study also revealed that the mortality for this model is high (>50%). Delgado-Roche *et al*. (2014) induced DCM in a rat model with intraperitoneal doxorubicin at 1 mg/kg twice a week for six weeks. However, in their study, they did not evaluate survival as a major endpoint. Gava *et al*. (2013) induced DCM in a rabbit model with intraperitoneal doxorubicin at 1 mg/kg twice a week for six weeks. They found that doxorubicin induced pathology in the left and right ventricles, and concluded that administration at a dose of 1 mg/kg twice a week for six weeks is safe and sufficient to induce DCM in rabbits. The aim of the present study was to compare the standard administration protocol with the new administration protocol, which each had the same cumulative dose, but were divided into more frequent administrations, aiming to determine whether DCM would continue to occur, but with reduced mortality.

2 Materials and methods

2.1 Animal model and grouping

A total of 150 male Sprague-Dawley (SD) rats (eight weeks old, weighing 250–280 g) were randomized into three experimental groups, which consisted of 50 rats each: the control group, which received saline (0.9% (9 g/L) NaCl) by intraperitoneal injection; the Dox 1 group, which received doxorubicin by intraperitoneal injection at a dose of 1 mg/kg twice a week for six weeks; Dox 2 group, received doxorubicin by intraperitoneal injection at a dose of 2 mg/kg once a week for six weeks. Rats were treated for six weeks, and observed for two weeks. All animals were sacrificed eight weeks after the treatments were started, when the rats were four months of age.

2.2 Echocardiography

At four months of age, the rats were anesthetized with 10% chloral hydrate (3 ml/kg, intraperitoneal). Body hair was removed by shaving the chest region, and echocardiography was performed to assess cardiac morphology and function using a Philips CX50 ultrasound (Royal Dutch Philips Electronics Ltd., Amsterdam, Dutch) with a 12-MHz transducer. Images were gated to the electrocardiogram. A parasternal short axis view in the middle of the left ventricle (LV) at the level of papillary muscles was used for analysis. The LV end-systolic diameter (LVESD) and end-diastolic diameter (LVEDD) were measured. Fractional shortening (FS) was calculated as (LVEDD−LVESD)/LVEDD×100%, and was calculated as a percentage (%). LV ejection fraction (LVEF) was calculated from the dimension values as ($LVEDD^3$−$LVESD^3$)/$LVEDD^3$×100%, and was calculated as a percentage (%). For each variable, images from three cardiac cycles were analyzed and averaged for each rat.

2.3 Plasma BNP and CRP, and serum CREA and AST

Twelve hours after echocardiography acquisition, uncoagulated blood was collected from the orbital venous plexus, anticoagulated with ethylene diamine tetraacetic acid (EDTA), and centrifuged at 13 000 r/min for 10 min. Serum was stored at −80 °C until further testing. Plasma brain natriuretic peptide (BNP) and C-reactive protein (CRP) concentrations were measured by enzyme-linked immunosorbent assay (ELISA), according to the manufacturer's instructions. Serum creatinine (CREA) and aspartate aminotransferase (AST) concentrations were measured by ELISA.

2.4 Caspase-3 mRNA analysis

Animals were euthanized with KCl (2 mol/L, intravenous). The heart was removed and rinsed with phosphate buffered saline (PBS), followed by the removal of the LV free wall. The excised myocardium was sliced into sections, and one section was snap-frozen at −80 °C for mRNA evaluation by quantitative real-time polymerase chain reaction (PCR). The housekeeping gene *β-actin* was used as a reference gene. The gene sequences used are shown in Table 1.

Table 1 Sequences of target gene *HMGB1* and *β-actin*

Name	Sequence (5'→3')	Product (bp)
HMGB1	F: CTGGACTGCGGTATTGAG	102
	R: GGGTGCGGTAGAGTAAGC	
β-actin	F: GACAACTTTGGCATCGTGGA	
	R: ATGCAGGGATGATGTTCTGG	

F: forward; R: reverse

2.5 Histological analysis

Autopsy was performed on all animals that died before completing the study protocol. Surviving animals were euthanized with KCl (2 mol/L, intravenous). The heart was removed and rinsed with PBS, the septal wall myocardial tissue was fixed in 10% formalin and embedded in paraffin, and the sections (5 μm thick) were evaluated with hematoxylin and eosin (H & E) staining for microscopic observation. Animals that survived until the end of the study protocol were included in the histological analysis.

2.6 Myocardial metabolism imaging by ^{18}FDG-PET/computed tomography (CT)

Positron emission tomography (PET) has been used to monitor LV dilation in rats (Stegger *et al*., 2005; Handa *et al*., 2007). The Siemens Inveon P120 PET scanner (Siemes, Inveon Dedicate, Germany) was used for PET imaging. The rats were fasted and water was withheld for 8 h before imaging to prevent interference from glucose during the imaging. After placing a catheter into the tail vein, rats were anesthetized with 10% chloral hydrate (3 ml/kg, intraperitoneal). The rats were positioned in the prone position within the PET scanner, and were kept warm with a heating pad. Core body temperature was maintained at 37 °C through the continuous monitoring of rectal temperature. After the intravenous administration of 2-deoxy-2-(^{18}F)fluoro-D-glucose (FDG; (19±5) MBq), an electro-cardiogram (ECG)-gated emission recording followed throughout the interval 60–90 min after tracer injection, and was concluded by a 7-min transmission scan as previously described, which was obtained to assess myocardial viability (Gava *et al*., 2013). Standard uptake value was defined using the following formula: intensity of the radioactivity of the region of interest (MBq/ml)/(radioactivity intensity of injected ^{18}FDG (MBq)×body weight (g)).

2.7 Statistical analysis

All data were processed with SPSS 21.0 software (Statistical Product and Service Solutions, Chicago, USA) and expressed as mean±standard deviation (SD). Kaplan-Meier analysis was performed to determine differences in survival rates. For parametric data, repeated measures analysis of variance (ANOVA) was used to compare the body weight in the four groups, and one-way ANOVA was used for the remaining continuous variables. When a statistically significant difference was observed among groups, a least significant difference test or Dunnett's test was performed. A P-value of <0.05 was considered statistically significant.

3 Results

3.1 General state of health

In Dox 1 and Dox 2 treated rats, body hair was ruffled and alopecia occurred. In addition, physical activity was reduced, and the rats ingested less food. Body weight was significantly reduced by the third week of injection, and the reduction in body weight was greater in the Dox 2 group than in the Dox 1 group (Fig. 1).

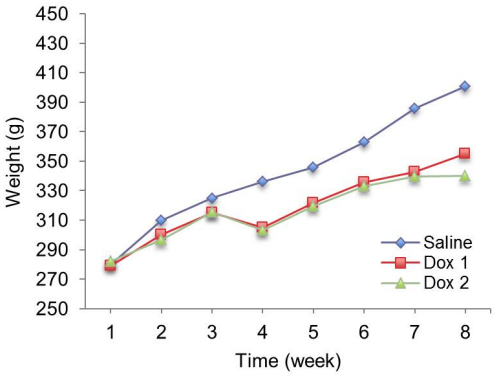

Fig. 1 Changes of body weight in three groups
Values are presented as mean±standard deviation

3.2 Mortality

There were no deaths in the saline-treated vehicle control group throughout the experiment, which was expected. Twenty-two percent (11/50) of the rats died in the Dox 1 group, while 48% (24/50) of rats

died in the Dox 2 group (P<0.001, by Kaplan-Meier analysis). Deaths were attributed to acute heart failure, serious gastrointestinal tract hemorrhage, or sudden cardiac death (Fig. 2).

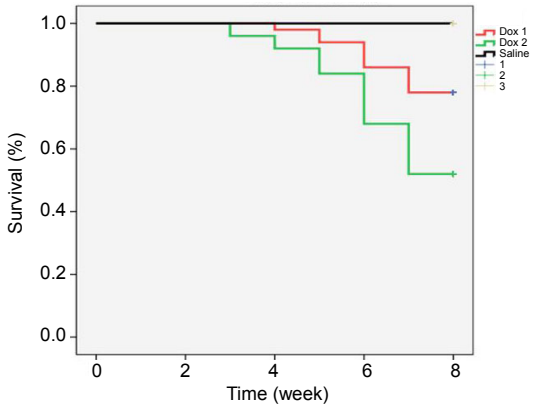

Fig. 2 Survival rate in three groups

Survival rate in the Dox 1 group was 78%, while mortality in the Dox 2 group was 52% (P<0.001)

3.3 Echocardiography

Significant LV chamber dilatation was present in the Dox 1 and Dox 2 groups, compared to the control group, as evidenced by increased LVEDD and LVESD. As a result, there was a significant reduction in systolic function in the Dox 1 and Dox 2 groups, with decreased LVEF and FS (Table 2, Fig. 3).

3.4 Plasma BNP

Plasma BNP levels were significantly higher in the Dox 1 and Dox 2 groups, compared with the control group (Table 3, Fig. 4; P<0.05 for both vs. the control group), which was consistent with the development of congestive heart failure.

3.5 Caspase-3 mRNA

Caspase-3 mRNA was significantly higher in the myocardium of rats in the Dox 1 and Dox 2 groups

Table 2 Echocardiographic findings at Week 8

Group	Number	HR (bpm)	LVEDD (mm)	LVESD (mm)	LVEF (%)	FS (%)
Saline	50	403±31	5.30±0.79	2.30±0.30	89±30	57±35
Dox 1	41	398±36	6.07±0.68*	3.93±0.33*	72±46*	37±33*
Dox 2	26	402±45	6.02±0.59*	3.89±0.28*	73±40*	33±29*

Values are presented as mean±standard deviation. * P<0.05, vs. saline vehicle control. HR: heart rate; bpm: beat per minute; LVEDD: left ventricle end-diastolic diameter; LVESD: left ventricle end-systolic diameter; LVEF: left ventricle ejection fraction; FS: fractional shortening

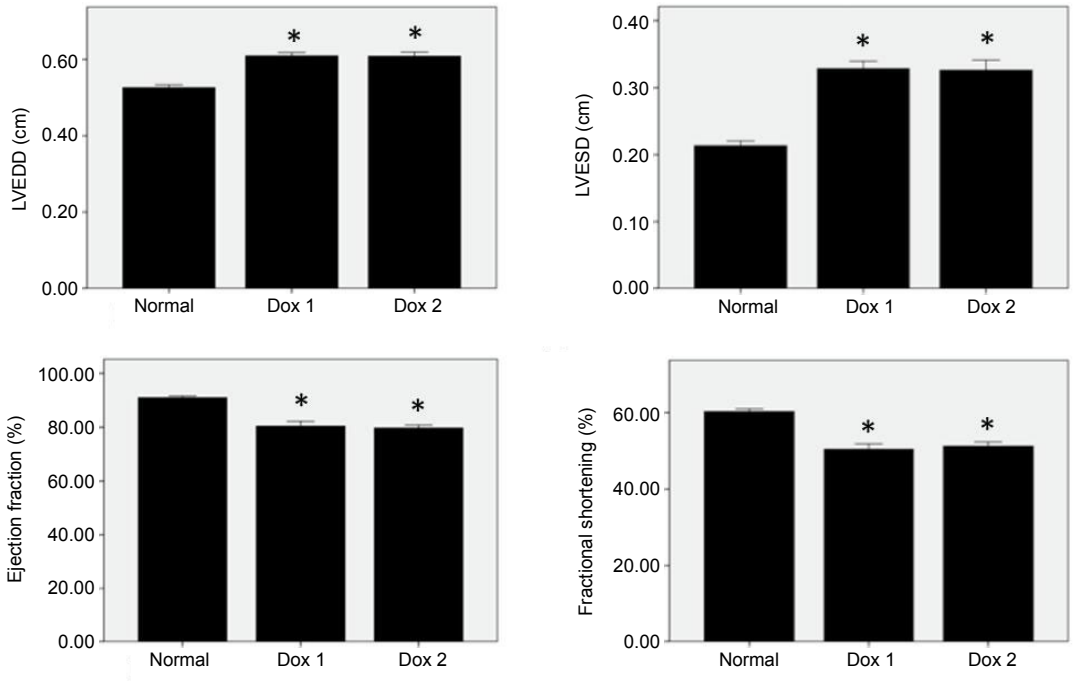

Fig. 3 Echocardiography changes in three groups

Values are presented as mean±standard deviation. * P<0.05, vs. the control normal group. LVEDD: left ventricle end-diastolic diameter; LVESD: left ventricle end-systolic diameter

Table 3 Plasma BNP levels at Week 8

Group	Number	BNP (pg/ml)
Saline	50	289±17
Dox 1	41	468±133*
Dox 2	26	497±99*

Values are presented as mean±standard deviation. * P<0.05, vs. saline vehicle control. BNP: brain natriuretic peptide

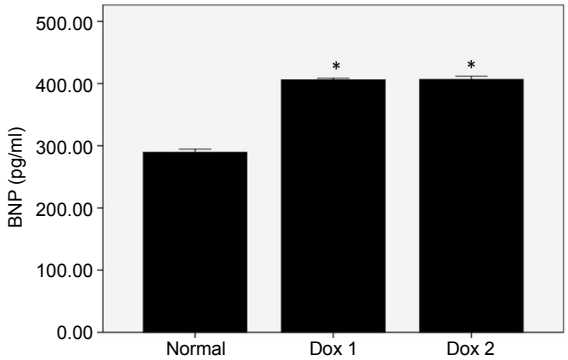

Fig. 4 Changes of plasma brain natriuretic levels in three groups

Values are presented as mean±standard deviation. * P<0.05 vs. the control group. BNP: brain natriuretic peptide

than of rats in the control group (Table 4, Fig. 5; P<0.05 for both vs. the control group).

3.6 Histological analysis

Myocardial samples collected from rats in the control group revealed no histopathological changes, as expected. Myocardial samples obtained from the Dox 1 and Dox 2 groups revealed extensive cardiomyocyte vacuolization, degeneration and necrosis, interstitial edema, inflammatory cell infiltration, and replacement fibrosis (Fig. 6).

3.7 Myocardial metabolism imaging by ^{18}FDG-PET/CT

Myocardial metabolism imaging by ^{18}FDG-PET/CT revealed a significant decrease in standard uptake values for FDG uptake, indicating reduced myocardial viability in both Dox 1 and Dox 2 groups (Table 5, Fig. S1).

3.8 Serum CREA and AST, and plasma CRP

Serum CREA and AST, and plasma CRP levels were significantly higher in the Dox 1 and Dox 2 groups than in the control group. Serum CREA and AST, and plasma CRP levels were significantly higher in the Dox 2 group than the Dox 1 group (Table 6, Figs. 7 and 8).

Table 4 Caspase-3 mRNA expression at Week 8

Group	Number	Caspase-3
Saline	50	0.79±0.29
Dox 1	41	1.39±0.48*
Dox 2	26	1.38±0.50*

Values are presented as mean±standard deviation. * P<0.05, vs. saline vehicle control

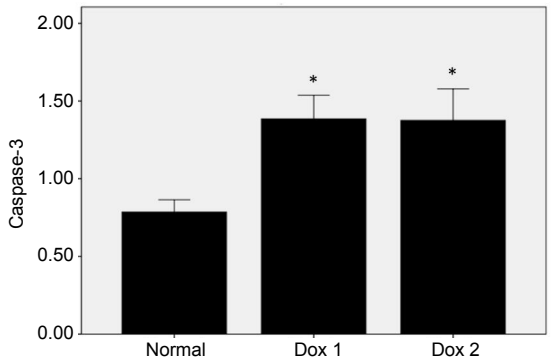

Fig. 5 Changes of Caspase-3 mRNA in three groups

Values are presented as mean±standard deviation. * P<0.05, vs. the control normal group

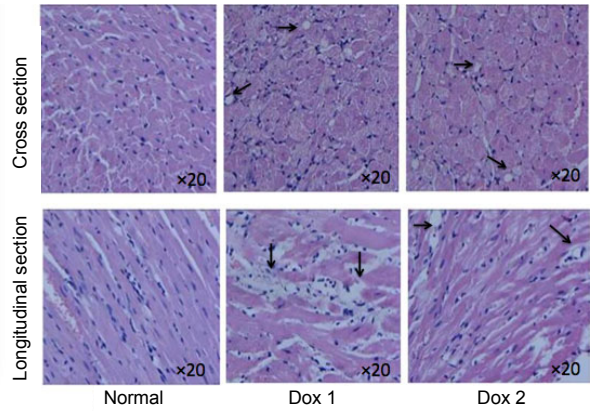

Fig. 6 Histolopathological analysis

Representative hematoxylin and eosin stained sections for the control group (left), Dox 1 (middle), and Dox 2 (right); both cross section (upper) and vertical section (lower). The control group revealed no histopathological changes. Myocardial samples from the Dox 1 and Dox 2 groups revealed vacuolization, interstitial edema, degeneration, necrosis, inflammatory cell infiltration and fibrosis (10×20 magnification)

Table 5 Standard FDG uptake values (SUV) in the myocardium at Week 8

Group	Number	SUV
Saline	50	9.4±2.1
Dox 1	41	5.8±1.0*
Dox 2	26	5.7±1.2*

Values are presented as mean±standard deviation. * P<0.05, vs. saline vehicle control

Table 6 Serum creatinine, aspartate aminotransferase (AST), and plasma C-reactive protein (CRP) levels at Week 8

Group	Number	Creatinine (μmol/L)	AST (U/L)	CRP (ng/ml)
Saline	50	23.8±3.7	119.4±4.2	31.9±3.4
Dox 1	41	64.0±10.3*	202.6±37.1*	43.4±2.1*
Dox 2	26	97.1±6.1*Δ	272.0±13.3*Δ	55.1±4.6*Δ

Values are presented as mean±standard deviation. * P<0.01, vs. saline vehicle control; Δ P<0.01, vs. Dox 1

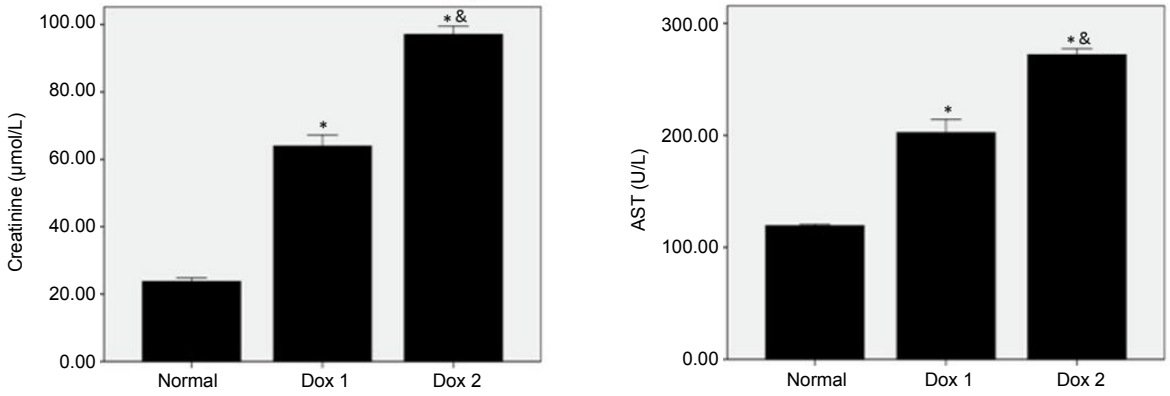

Fig. 7 Changes of serum creatinine (CREA) and aspartate aminotransferase (AST) levels in three groups
Values are presented as mean±standard deviation. * P<0.05, vs. the control group; & P<0.01, vs. Dox 1

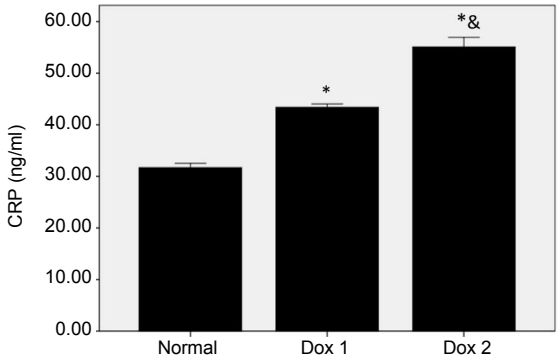

Fig. 8 Changes of plasma CRP levels in three groups
Values are presented as mean±standard deviation. * P<0.05, vs. the control group; & P<0.01, vs. Dox 1. CRP: C-reactive protein

4 Discussion

The goal of this study was to compare different administration times (once a week vs. twice a week) of doxorubicin, and to establish the rat DCM model that reduces animal usage. The major findings of this study revealed that the twice a week injection of 1 mg/kg for six weeks could generate LV dilation, reduce myocardial viability, and induce histopathological changes, which is consistent with DCM. Furthermore, these results indicate that doxorubicin can be used in rats at a concentration that induces DCM, while more than doubling the survival rate. This model would be useful for mechanistic studies in exploring causes and consequences of chemotherapy-induced cardiotoxicity.

Several other laboratories have used similar protocols to generate DCM models using doxorubicin injection. Yu *et al*. (2013) used a dose of 2.5 mg/kg of doxorubicin, which was intravenously administered twice a week for eight weeks. Other studies (Leontyev *et al*., 2013) used 2.5 mg/kg doses administered by intraperitoneal injection once a week for six weeks. Gu *et al*. (2012) induced DCM in a rat model using six equal doses of intraperitoneal doxorubicin, for a total dose of 15 mg/kg, which was administered for over two weeks. However, due to the leakage of doxorubicin from the intravenous injection, many of these protocols resulted in serious phlebitis, and even blocked blood vessels, which contributed to increased morbidity and mortality through mechanisms that are not clinically relevant. Although some researchers did not report the mortality rates in their studies, this study, as well as other studies, have reported high mortality that exceeded 50% for these protocols (Ishida *et al*., 2004; Baba *et al*., 2007; Iwata *et al*., 2013). The author has previously reported a mortality rate of 54% when doxorubicin was injected intraperitoneally

at doses of 2 mg/kg once a week in rats. Gu *et al*. (2012) induced DCM in a rabbit model with intraperitoneally administered doxorubicin (1 mg/kg, twice a week) for six weeks, and demonstrated that this method is safe and sufficient to induce DCM in rabbits. This is the reason the author used a similar protocol in rats.

Doxorubicin is associated with a dose-dependent cardiotoxicity that can progress to heart failure, and the administration of doses over 1 mg/kg results in worse survival rates and classic signs of DCM (Hayward and Hydock, 2007). In the present study, the investigators found that the administration of 1 mg/kg twice weekly in rats was safe and without high mortality rates, allowing reliable assessments at the end of the study. Similar to humans and other animal models, the toxic potential of doxorubicin in rats depends on the dose administered and the time course of administration (e.g. once or twice weekly). The high mortality in the Dox 2 group can be explained by the high toxicity potential of the drug in several organs. Nephrotoxicity, hepatotoxicity, and myelosuppression are noted as side effects in addition to its well-described cardiotoxicity effects, which limit the use of doxorubicin (Kalender *et al*., 2005; Bardi *et al*., 2007). Our findings are consistent with previous research results. In the present study, plasma CREA and AST levels were significantly higher in rats administered weekly with doxorubicin at 2 mg/kg, indicating that nephrotoxicity and hepatotoxicity are more serious with a one-time dose. Anthracyclines significantly produce reactive free radicals that are capable of damaging cell membranes and DNA (Jones *et al*., 2006; Deng *et al*., 2009; Lu *et al*., 2009; Octavia *et al*., 2012). Thus, this drug exerts time- and dose-dependent toxicity in several organs (El-Sayyad *et al*., 2009).

CRP is an acute-phase protein, which has been found to be expressed in cardiomyocytes, endothelial cells, and microvascular endothelial cells in patients with DCM (Satoh *et al*., 2005). CRP can induce myocardial injury by activating the complement system and inducing leukocyte chemotaxis (Zimmermann *et al*., 2009). In DCM patients, elevated CRP was associated with inflammation and cardiac insufficiency (Mamamtavrishvili *et al*., 2008). In the present study, plasma CRP levels were significantly higher in rats in the Dox 2 group, and had a high mortality.

The present study investigated the mechanism of the cardiomyocyte apoptosis involved in myocardial injury during the development of DCM (Kawano *et al*., 1994; Haider *et al*., 1995). The cysteine aspartate protein (caspase) family includes functional proteases that regulate cell apoptosis, remodeling, and differentiation (Nicholson and Thornberry, 1997; Cryns and Yuan, 1998; Thornberry and Lazebnik, 1998). Caspase-3 is a critical upstream protein that initiates the apoptosis pathway (Faleiro *et al*., 1997; Martins *et al*., 1997; Polverino and Patterson, 1997). The activation of Caspase-3 occurs at early time points (1–24 h), as well as during the heart failure stage in the adriamycin (ADR)-induced cardiomyopathy model (Lou *et al*., 2005). The expression of pro-apoptotic protein Caspase-3 was significantly higher in the ADR-induced DCM model (Liu *et al*., 2012). The results of the current study are consistent with what others have reported, in which Caspase-3 mRNA was significantly elevated in the myocardium of rats treated with doxorubicin.

Echocardiography revealed that LV chamber dilatation, evidenced by enlarged LVEDD and LVESD, was translated to decreased fractional shortening and ejection fraction. These results were consistent with a previous report (Leontyev *et al*., 2013). Histopathological analysis and ^{18}FDG-PET myocardial metabolism imaging confirmed the cardiotoxic effects of doxorubicin in rats. Cardiomyocyte damages, leading to necrosis, edema, inflammatory cell infiltration, and fibrosis, were similar in both models. Similarly, ^{18}FDG-PET myocardial metabolism imaging revealed decreased myocardial viability, which was consistent with the findings reported by another study (Brunner *et al*., 2012). Similar to echocardiography, ^{18}FDG-PET imaging is a useful and minimally invasive evaluation method that can be used to detect pathological changes, offering the benefit of being useful for serial evaluations.

5 Conclusions

In conclusion, we compared two dosing regimens of doxorubicin in rats to determine a minimal protocol that can induce DCM, while improving survival. The administration of 1 mg/kg of doxorubicin twice a week for six weeks was found to be safe and sufficient for inducing DCM in rats.

Contributors

Li-juan SHEN carried out the molecular genetic studies, participated in the sequence alignment, and drafted the manuscript. Lan LI carried out the echocardiography. Qing-min XING carried out the immunoassays. Yong-liang XU participated in the sequence alignment. Yong-hua ZHOU participated in the design of the study and performed the statistical analysis. Shu LU conceived of the study, participated in its design and coordination, and helped to draft the manuscript. All authors read and approved the final manuscript.

Compliance with ethics guidelines

Li-juan SHEN, Shu LU, Yong-hua ZHOU, Lan LI, Qing-min XING, and Yong-liang XU declare that they have no conflict of interest.

All animal procedures were conducted in accordance with the Guide for the Care and Use of Laboratory Animals. Furthermore, the protocol was approved by the Animal Care and Use Committee of the Institute of Nanjing University of Chinese Medicine (Nanjing, China).

References

Baba, S., Heike, T., Yoshimoto, M., *et al*., 2007. Flk1^{+} cardiac stem/progenitor cells derived from embryonic stem cells improve cardiac function in a dilated cardiomyopathy mouse model. *Cardiovasc. Res.*, **76**(1):119-131. http://dx.doi.org/10.1016/j.cardiores.2007.05.013

Bardi, E., Bobok, I., Olah, A.V., *et al*., 2007. Anthracycline antibiotics induce acute renal tubular toxicity in children with cancer. *Pathol. Oncol. Res*., **13**(3):249-253. http://dx.doi.org/10.1007/BF02893506

Brunner, S., Todica, A., Boning, G., *et al*., 2012. Left ventricular functional assessment in murine models of ischemic and dilated cardiomyopathy using [^{18}F]FDG-PET: comparison with cardiac MRI and monitoring erythropoietin therapy. *EJNMMI Res*., **2**(1):43. http://dx.doi.org/10.1186/2191-219X-2-43

Carvalho, C., Santos, R.X., Cardoso, S., *et al*., 2009. Doxorubicin: the good, the bad and the ugly effect. *Curr. Med. Chem*., **16**(25):3267-3285. http://dx.doi.org/10.2174/092986709788803312

Cryns, V., Yuan, J., 1998. Proteases to die for. *Genes Dev.*, **12**(11):1551-1570. http://dx.doi.org/10.1101/gad.12.11.1551

Delgado-Roche, L., Hernandez-Matos, Y., Medina, E.A., *et al*., 2014. Ozone-oxidative preconditioning prevents doxorubicin-induced cardiotoxicity in Sprague-Dawley Rats. *Sultan Qaboos Univ. Med. J.*, **14**(3):e342-e348.

Deng, S., Kruger, A., Schmidt, A., *et al*., 2009. Differential roles of nitric oxide synthase isozymes in cardiotoxicity and mortality following chronic doxorubicin treatment in mice. *Naunyn-Schmiedeberg's Arch. Pharmacol*., **380**(1):25-34. http://dx.doi.org/10.1007/s00210-009-0407-y

El-Sayyad, H.I., Ismail, M.F., Shalaby, F.M., *et al*., 2009. Histopathological effects of cisplatin, doxorubicin and 5-flurouracil (5-FU) on the liver of male albino rats. *Int. J. Biol. Sci*., **5**(5):466-473. http://dx.doi.org/10.7150/ijbs.5.466

Faleiro, L., Kobayashi, R., Fearnhead, H., *et al*., 1997. Multiple species of CPP32 and MCh2 are the major active Caspases present in apoptotic cells. *EMBO*, **16**(9):2271-2281. http://dx.doi.org/10.1093/emboj/16.9.2271

Gava, F.N., Zacche, E., Ortiz, E.M., *et al*., 2013. Doxorubicin induced dilated cardiomyopathy in a rabbit model: an update. *Res. Vet. Sci.*, **94**(1):115-121. http://dx.doi.org/10.1016/j.rvsc.2012.07.027

Gu, R., Bai, J., Ling, L., *et al*., 2012. Increased expression of integrin-linked kinase improves cardiac function and decreases mortality in dilated cardiomyopathy model of rats. *PLoS ONE*, **7**(2):e31279. http://dx.doi.org/10.1371/journal.pone.0031279

Haider, N., Narula, J., Hajjar, R.J., *et al*., 1995. Apoptosis in human explanted cardiomyopathic hearts suggests programmed progression of dilatedcardiomyopathy. *Circulation*, **92**(8):3479-3479.

Handa, N., Magata, Y., Mukai, T., *et al*., 2007. Quantitative FDG-uptake by positron emission tomography in progressive hypertrophy of rat hearts in vivo. *Ann. Nucl. Med*., **21**(10):569-576. http://dx.doi.org/10.1007/s12149-007-0067-2

Hayward, R., Hydock, D.S., 2007. Doxorubicin cardiotoxicity in the rat: an in vivo characterization. *J. Am. Assoc. Lab. Anim. Sci*., **46**(4):20-32.

Ishida, M., Tomita, S., Nakatani, T., *et al*., 2004. Bone marrow mononuclear cell transplantation had beneficial effects on doxorubicin-induced cardiomyopathy. *J. Heart Lung Transplant*., **23**(4):436-445. http://dx.doi.org/10.1016/S1053-2498(03)00220-1

Iwata, Y., Ohtake, H., Suzuki, O., *et al*., 2013. Blockade of sarcolemmal TRPV2 accumulation inhibits progression of dilated cardiomyopathy. *Cardiovasc. Res*., **99**(4):760-768. http://dx.doi.org/10.1093/cvr/cvt163

Jones, R.L., Swanton, C., Ewer, M.S., 2006. Anthracycline cardiotoxicity. *Expert Opin. Drug Saf*., **5**(6):791-809. http://dx.doi.org/10.1517/14740338.5.6.791

Kalender, Y., Yel, M., Kalender, S., 2005. Doxorubicin hepatotoxicity and hepatic free radical metabolism in rats. The effects of vitamin E and catechin. *Toxicology*, **209**(1):39-45. http://dx.doi.org/10.1016/j.tox.2004.12.003

Kawano, H., Okada, R., Kawano, Y., *et al*., 1994. Apoptosis in acute and chronic myocarditis. *Jpn. Heart*, **35**(6):745-750. http://dx.doi.org/10.1536/ihj.35.745

Leontyev, S., Schlegel, F., Spath, C., *et al*., 2013. Transplantation of engineered heart tissue as a biological cardiac assist device for treatment of dilated cardiomyopathy. *Eur. J. Heart Fail*., **15**(1):23-35. http://dx.doi.org/10.1093/eurjhf/hfs200

Liu, H.Z., Gao, C.Y., Wang, X.Q., *et al*., 2012. Angiotensin(1-7) attenuates left ventricular dysfunction and myocardial apoptosis on rat model of adriamycin-induced dilated cardiomyopathy. *Chin. J. Cardiol*., **40**(3):219-224 (in Chinese).

Lou, H., Danelisen, I., Singal, P.K., 2005. Involvement of mitogen-activated protein kinases in adriamycin-induced cardiomyopathy. *Am. J. Physiol. Heart Circ. Physiol*., **288**(4):H1925-H1930. http://dx.doi.org/10.1152/ajpheart.01054.2004

Lu, L., Wu, W., Yan, J., *et al*., 2009. Adriamycin-induced autophagic cardiomyocyte death plays a pathogenic role in a rat model of heart failure. *Int. J. Cardiol*., **134**(1): 82-90. http://dx.doi.org/10.1016/j.ijcard.2008.01.043

Mamamtavrishvili, N.D., Kvirkveliia, A.A., Abashidze, R.I., *et al*., 2008. Role of immune inflammatory activity in chronic heart failure progress. *Georgian Med. News*, **160/161**:30-34.

Martins, L.M., Kottke, T., Mesner, P.W., *et al*., 1997. Activation of multiple interleukin 1 β-bconverting enzyme homologues in cytosol and nuclei of HL-60 cells during etoposideinduced apoptosis. *J. Biol. Chem.*, **272**(11): 7421-7430. http://dx.doi.org/10.1074/jbc.272.11.7421

Nicholson, D.W., Thornberry, A., 1997. Caspase: killer proteases. *Trends Biochem. Sci.*, **22**(8):299-306. http://dx.doi.org/10.1016/S0968-0004(97)01085-2

Octavia, Y., Tocchetti, C.G., Gabrielson, K.L., *et al*., 2012. Doxorubicin-induced cardiomyopathy: from molecular mechanisms to therapeutic strategies. *J. Mol. Cell. Cardiol*., **52**(6):1213-1225. http://dx.doi.org/10.1016/j.yjmcc.2012.03.006

Plana, J.C., Galderisi, M., Barac, A., *et al*., 2014. Expert consensus for multimodality imaging evaluation of adult patients during and after cancer therapy: a report from the American Society of Echocardiography and the European Association of Cardiovascular Imaging. *Eur. Heart J. Cardiovasc. Imaging*, **15**(10):1063-1093. http://dx.doi.org/10.1093/ehjci/jeu192

Polverino, A.J., Patterson, S.D., 1997. Selective activation of caspases during apoptotic induction in HL-60 cells. *J. Biol. Chem.*, **272**(11):7013-7021. http://dx.doi.org/10.1074/jbc.272.11.7013

Satoh, M., Nakmura, M., Akatsu, T., *et al*., 2005. C-reactive protein co-expresses with tumor necrosis factor-α in the myocardium in human dilated cardiomyopathy. *Eur. J. Heart Fail.*, **7**(5):748-754. http://dx.doi.org/10.1016/j.ejheart.2004.10.018

Stegger, L., Schafers, K.P., Flogel, U., *et al*., 2005. Monitoring left ventricular dilation in mice with PET. *J. Nucl. Med*., **46**(9):1516-1521.

Thornberry, N.A., Lazebnik, Y., 1998. Caspase: enemies within. *Science*, **281**(5381):1312-1316. http://dx.doi.org/10.1126/science.281.5381.1312

Turakhia, S., Venkatakrishnan, C.D., Dunsmore, K., *et al*., 2007. Doxorubicin-induced cardiotoxicity: direct correlation of cardiac fibroblast and H9c2 cell survival and aconitase activity with heat shock protein 27. *Am. J. Physiol. Heart Circ. Physiol*., **293**(5):H3111-H3121. http://dx.doi.org/10.1152/ajpheart.00328.2007

Vejpongsa, P., Yeh, E.T., 2014. Prevention of anthracycline-induced cardiotoxicity: challenges and opportunities. *J. Am. Coll. Cardiol*., **64**(9):938-945. http://dx.doi.org/10.1016/j.jacc.2014.06.1167

Yu, S.Y., Liu, L., Li, P., *et al*., 2013. Rapamycin inhibits the mTOR/p70S6K pathway and attenuates cardiac fibrosis in adriamycin-induced dilated cardiomyopathy. *Thorac. Cardiovasc. Surg*., **61**(3):223-228. http://dx.doi.org/10.1055/s-0032-1311548

Zimmermann, O., Bienek-Ziolkowski, M., Wolf, B., *et al*., 2009. Myocardial inflammation and non-ischaemic heart failure: is there a role for C-reactive protein? *Basic Res. Cardiol*., **104**(5):591-599. http://dx.doi.org/10.1007/s00395-009-0026-2

List of electronic supplementary materials

Fig. S1 Myocardial metabolism imaging by ^{18}FDG-PET/CT

中文概要

题　目：提高扩张型心肌病动物模型的生存率

目　的：比较在腹腔注射相同剂量阿霉素（12 mg/kg）下，不同给药方案构建扩张型心肌病大鼠模型的生存率。

创新点：首次应用腹腔注射阿霉素 1 mg/kg，一周两次的方法构建扩张型心肌病大鼠模型，并与常规的方法进行生存率的比较。

方　法：将 150 只 SD 雄鼠分为对照组（腹腔注射生理盐水）、Dox 1 组（腹腔注射阿霉素 1 mg/kg 一周两次，共六周）和 Dox 2 组（腹腔注射阿霉素 2 mg/kg 一周一次，共六周）。观察及比较各组大鼠的体重、生存率、心腔大小、pro-BNP、CRP、CREA、AST 和 Caspase-3 mRNA 水平。观察各组大鼠心肌病理变化，同时进行 ^{18}FDG-PET 心肌代谢显像。

结　论：本实验中结果显示，Dox 1 组和 Dox 2 组在 pro-BNP、Caspase-3 mRNA 水平、心肌病理变化及 ^{18}FDG-PET 心肌代谢显像上均没有明显差异；但 Dox 1 组的生存率是 78%，而 Dox 2 组的生存率是 52%；同时，Dox 2 组大鼠的血清 CREA、AST 和 CRP 水平比 Dox 1 组明显升高。综上所述，腹腔注射阿霉素 1 mg/kg 一周两次的方法在成功构建扩张型心肌病大鼠模型的同时大大提高了存活率。

关键词：阿霉素；扩张型心肌病；动物模型；^{18}FDG-PET